Liquid sensing: smart polymer/CNT composites

Today polymer/carbon nanotube (CNT) composites can be found in sports equipment, cars, and electronic devices. The growth of old and new markets in this area has been stimulated by our increased understanding of relevant production and processing methods, as well as the considerable price reduction of industrial CNT grades. In particular, CNT based electrically conductive polymer composites (CPCs) offer a range of opportunities because of their unique property profile; they demonstrate low specific gravity in combination with relatively good mechanical properties and processability. The electrical conductivity of polymer/CNT composites results from a continuous filler network that can be affected by various external stimuli, such as temperature shifts, mechanical deformations, and the presence of gases and vapors or solvents. Accordingly, CNT based CPCs represent promising candidates for the design of smart components capable of integrated monitoring. In this article we focus on their use as leakage detectors for organic solvents.

Tobias Villmow, Sven Pegel, Andreas John, Rosina Rentenberger, and Petra Pötschke*
Leibniz Institute of Polymer Research Dresden, Hohe Strasse 6, 01069 Dresden, Germany
**E-mail: poe@ipfdd.de*

Since the first research was performed in this field using carbon black (CB), it has been well known that conductive polymer composites (CPCs) are sensitive to external stimuli. Environmental factors such as the presence of liquids[1-5] and vapors[6-11] were found to significantly change the electrical resistivity of CPCs. In the early 1990s a large amount of research focused on using carbon nanotubes (CNTs) as a filler for CPCs[12]. One of the advantages of using CNTs in composite materials is the relatively low percolation threshold that can be achieved, due to the high length/diameter ratio (aspect ratio) of up to 1000. Thus, polymer/CNT composites exhibit high mechanical strength and stiffness combined with electrical conductivity at relatively low CNT concentrations[13,14].

Design concepts and capabilities

Numerous different designs of sensory CPCs containing CNTs have previously been proposed[15]. For example, partially embedded CNTs in

ISSN:1369 7021

a polymer matrix[16] (Fig. 1a), CNTs arranged in a dense network placed on polymer surfaces or fibers[17] (Fig. 1b), and fully embedded CNTs in a polymer matrix[18-28] (Fig. 1c) have all been made. Solution casting of polymer-nanotube dispersions in suitable solvents is one possible method of producing thin film[16,19-22] or layer-by-layer assembly sensors[18]. Such dispersions could be used to impregnate non-conductive textiles or plastic parts with sensory CPC coatings.

In the context of large-scale processing of sensory CPCs, fully embedded CNTs show the most potential, as these materials can be realized using cost efficient and tailored melt processing techniques, such as injection or compression molding[23,24,28], blow molding, and fiber spinning[25-27]. Besides the multiplicity of possible shaping techniques, CPCs containing CNTs may be processed into various shapes and sizes (some examples are shown in Fig. 1d). In particular, CPCs containing CNTs offer advantages for the production of fibers, as their spinnability processing window is much broader compared to, e.g., CB filled systems[25,29-32].

The sensing mechanism of CPCs is based on the polymer's reaction to environmental changes which affect the electrically conductive CNT network. External stimuli such as temperature shifts, mechanical deformations, and the presence of gases and vapors or solvents result in measurable resistance changes of the CPC. For instance, below the glass transition temperature, T_g, the mismatch between the coefficients of thermal expansion of the CNTs and the matrix leads to a positive[33,34] or negative[35-37] temperature coefficient of resistance (PTC and NTC), resulting in an increase or decrease of the composite resistance with temperature. A disproportionately high change of resistance was found near T_g[33,34,37]. The electrical response of CPCs to mechanical stresses is explained by the increasing distance between individual CNTs exceeding the tunneling distance under the applied load[38]. Swelling of the CPC due to contact with organic vapors[16-22] or liquids[23-28] also results in the local disconnection of electrical contacts between individual CNTs and/or CNT clusters, resulting in an increase of electrical resistance.

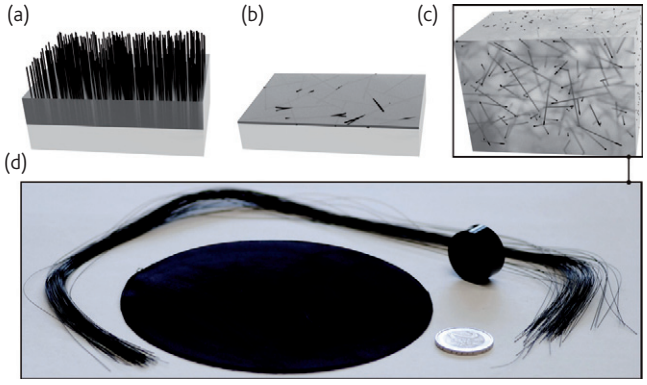

Fig. 1 Different sensory CPC designs and CNT arrangements. (a) Partially embedded CNTs in polymer, (b) a polymer substrate covered with CNTs, and (c) fully embedded CNTs in polymer. (d) Possible sensory CPC shapes (fibers, compression-molded plate, cylinder, and a €2 coin for size comparison).

The numerous designs and shapes of sensory CPCs, in combination with the ease with which they can be processed, make these materials an interesting class, with many possible applications.

Fundamentals of solvent detection

Mechanism

Using CPCs as sensory materials for the detection of organic solvents is based on the ability of polymeric materials to swell. If a solvent is able to diffuse into the polymer matrix of a CPC, the resulting expansion induces an increase in the nanotube-nanotube distance of neighboring CNTs, which reduces the tunneling current. Therefore, the resistivity of the filler network increases as the swelling process proceeds. Exceeding the critical tunneling distance, which is approximately 1.8 nm[39], results in the separation of individual CNTs and CNT clusters from the network. Both effects must be considered when discussing the relative change in resistance of CPCs on contact with "good" solvents.

The corresponding change of resistivity is thereby related to the local volumetric solvent take-up. Considering the case of a dry 3D CPC sensor sample dropped into a solvent, the swelling process will start at the surface and the resistivity will therefore be inhomogeneous over the cross-sectional area. Thus, for uniform filler content, the resistance of the sensor depends on its geometry, the penetration depth of solvent, and the direction of the current flow. The time dependency of the relative resistance change can be correlated with the diffusion kinetics of solvent molecules into the CPC[28].

The diffusion path $s(t)$ locally separates a swollen skin from the originally dry core. Fig. 2a shows a schematic of a partially swollen CPC sample. The skin and core regions, having different CNT network densities, are separated by a sharp solvent front, which can be visualized using transmission light microscopy[28]. The swelling leads to an expansion of the polymer matrix in the skin region and, thus, to a local reduction of the effective CNT content, and an increase of the contact distances. The total sample conductivity is a result of contributions from both the core and skin regions. The reduction of the core cross-section with increasing solvent penetration leads to a time dependent increase of the total sample resistance, until a plateau value is eventually reached.

Selectivity

The proposed mechanism is valid for CPCs in contact with "good" solvents. The attribute "good" refers to the ability of the solvent to eventually dissolve a specific polymer, where the initial stage of the dissolution process is the polymer swelling. When a solvent does not result in the swelling of the matrix, the solvent is described as "bad". The term "good" is therefore specific to a given polymer/solvent system. For this reason, the most important issue in the design of sensory CPCs is the choice of polymer component, as it governs the range of detectable organic solvents. The similarity of their solubility parameters determines whether a specific CPC will swell in a specific

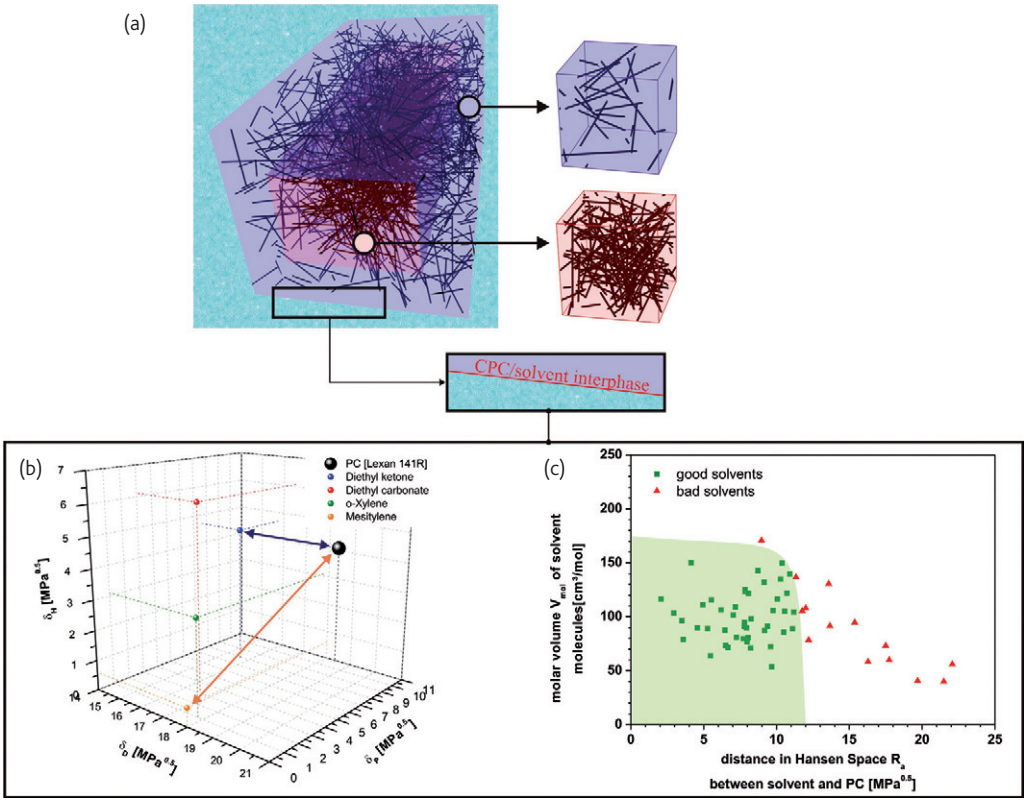

Fig. 2 Underlying mechanism for the relative electrical resistance change of CPCs in contact with "good" organic solvents. (a) Development of the skin-core morphology, showing (blue) the swollen skin and (brown) the dry core, with altered and original composite properties, respectively. (b) Plot of Hansen solubility parameters used for the description of the interaction at the CPC/solvent interface for polycarbonate (PC) with different solvents. (c) Solvent map indicating the CPC's selectivity, for the example of PC.

solvent, in accordance with the principle of "like dissolves like". The use of Hansen solubility parameters (HSP) presents a relatively clear method of quantifying the similarity of polymers and solvents. The solubility parameter δ (unit $MPa^{0.5}$), terminologically introduced by Hildebrand and Scott, is defined as the square root of the cohesive energy density of a given chemical compound[40,41]. Hansen further developed this concept by segmenting the solubility parameter into partial parameters, allowing the dispersive (δ_D), polar (δ_P), and hydrogen bonding (δ_H) contributions to be considered separately[42]. As an example, the location of a specific polycarbonate (PC Lexan 141R, Sabic) and four different organic solvents in the corresponding Hansen space is shown in Fig. 2b. This three-dimensional consideration allows the calculation of a solubility parameter distance R_a between the polymer and solvent that represents the strength of interaction. Basically, the partial solubility parameters of PC used in this figure are the centre point of a solubility sphere with a radius R_ϕ. Solvents located within this sphere will result in a polymer swelling and the final dissolution process. Solvents exceeding the critical R_a value will predominantly not dissolve the matrix and will therefore not result in a relative resistance change of CPCs based on this polymer.

Additional aspects which influence the solubility of polymers are the solvent molecule size and the temperature. Smaller molecule sizes or molar volumes V_{mol} can result in promoted swelling processes, although the distance in Hansen space regarding a specific polymer is rather large. Variations in temperature can lead to significantly different solubility behavior. The change of the Hansen solubility parameters of polymers and solvents with temperature depends on their thermal expansion coefficients. The most temperature sensitive partial parameter is the hydrogen bonding parameter, which decreases more rapidly than the others. Polymers also show an enlargement of their solubility sphere radius with increasing temperature[42]. This leads to the conclusion that a non-solving liquid can become a solving one with increasing temperature, and a non-solving one with greater temperatures. This was found to be especially true for solvent/polymer systems where the solvent is just outside the polymer's solubility sphere.

Fig. 2c presents a solvent map of the solvent selectivity of a CPC based on PC and 1.5 wt% multiwalled CNTs (MWCNTs), where all measurements were performed at room temperature. The selectivity is a function of the distance between the PC and the solvent in three-dimensional Hansen space, as well as the solvent's molar volume V_{mol}. Each spot on the map corresponds to a specific solvent. Green data points represent solvents that lead to significant and fast resistance increases of the CPC. Solvents marked with red dots do not lead to

relative resistance changes of the CPC. This solvent mapping allows the definition of the selectivity of the specific CPC; by constructing an area that may separate the good and bad solvents. Furthermore, it is possible to predict the relative resistance change upon contact with an untested "new" solvent from its HSP and molar volume.

The solubility parameters of the specific PC used in this study were calculated using the commercial software *Hansen solubility parameters in practice* based on solubility data obtained from sensing experiments, while the HSP of the organic solvents were taken from literature[42,43].

Electrical response characteristics

Organic liquids may be detected through resistance changes of CPCs if the liquid is a good solvent for the polymer component of the CPC. The electrical response characteristics depend on the diffusion kinetics of the specific solvent molecules in the CPC. The shape of the time dependence of the relative resistance change R_{rel} is therefore predominantly governed by the diffusion coefficient k. In the case of the Fickian mode of solvent molecule transport, the parameter k has units of $cm \cdot s^{-0.5}$. Larger k values promote solvent penetration and result in higher relative resistance change rates. The relative resistance change of a PC/MWCNT composite with 1.5 wt% MWCNT (for production see[28]) during immersion in different solvents is shown in Fig. 3a (experimental data are represented by grey symbols).

R_{rel} of different CPCs shows a similar progression with immersion time, and the behavior can be divided into three different stages. Stage I, at the beginning of the solvent immersion process, is characterized by a moderate increase of R_{rel} versus time. This period is attributed to the diffusion of solvent molecules into the bulk material. A sharp increase of R_{rel} can be allocated to a second stage, which is attributed to the convergence of solvent fronts which occurs in the middle of the samples. This increase can be of several orders of magnitude, depending on the MWCNT content. The convergence of solvent fronts results in stage III, where R_{rel} reaches a plateau value without further resistance change. The time t_p to reach the plateau is an important system parameter, as it enables the calculation of the diffusion coefficient k[28].

The electrical responses of CPCs vary significantly during immersion in different organic solvents. The different kinetics correlate with the diffusion kinetics of the solvent molecules in the CPC. A model allowing the calculation of the time dependent relative resistance change has been proposed considering several factors such as the diffusion parameters, composite characteristics, and geometrical values, and has been adapted for the example of PC with 1.5 wt% MWCNT, as named above[28]. Simulated R_{rel} curves, indicated by colored lines, for the same set of solvents, are shown in Fig. 3a. The experimentally determined and simulated data show a very high degree of agreement.

The time dependent relative resistance change is mostly affected by the diffusion coefficient k. The effect of some influencing factors on k is presented in Fig. 3b for PC/MWCNT composites. The influence of MWCNT content on the diffusion coefficient k is shown in Fig. 3b-I for PC/MWCNT composites immersed in ethyl acetate. Increasing the CNT content decreases the diffusion coefficient k, as "denser" CNT networks represent obstacles for the solvent molecules. The same trend was found by increasing the size of the solvent's molecules. Fig. 3b-II shows decreasing k values for different halogenated hydrocarbons, with increasing molar volume of the solvent molecules. This result indicates that a sensory CPC enables the distinct discrimination of different solvents in contact with the sample, as they result in different electrical response characteristics. The functional capability of sensory CPC is assured for a broad temperature range, where the upper limit is the service temperature of the polymer. The lower limit is governed by the flexibility of the CPC needed for the specific

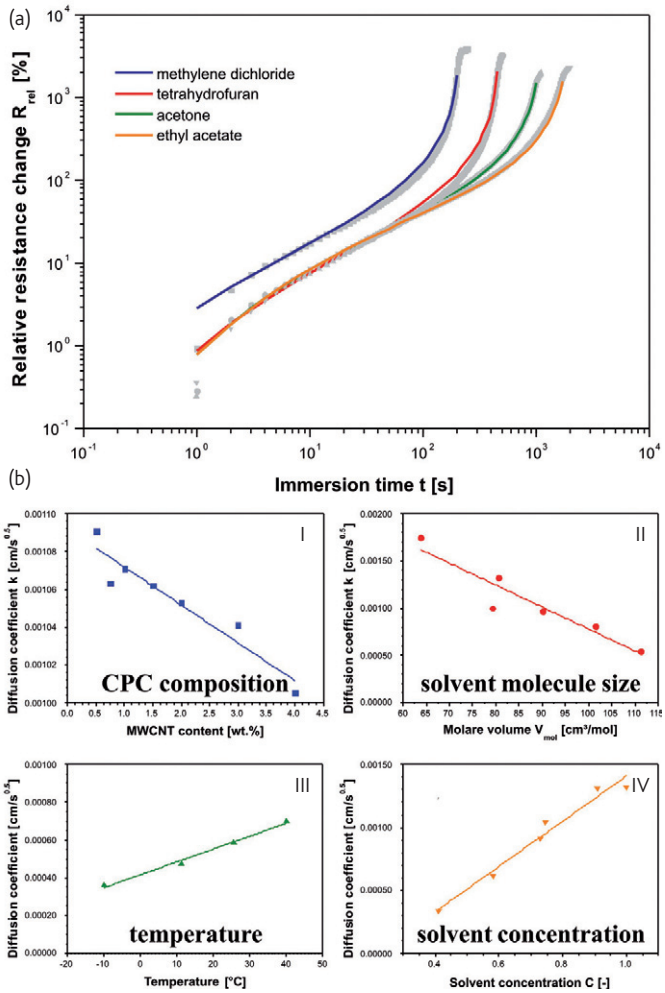

Fig. 3 (a) Electrical response characteristics of PC/MWCNT composites during immersion in different solvents, adapted from[28] with permission from Elsevier. (b) Influencing factors on the diffusion coefficient k that govern the progression of R_{rel} curves (for a CPC containing 1.5 wt.% MWCNT) (I) Influence of CPC composition; (II) influence of molecule size of six different halogenated hydrocarbons; (III) influence of temperature; and (IV) influence of solvent concentration for mixtures of chloroform with methanol and diethyl ether.

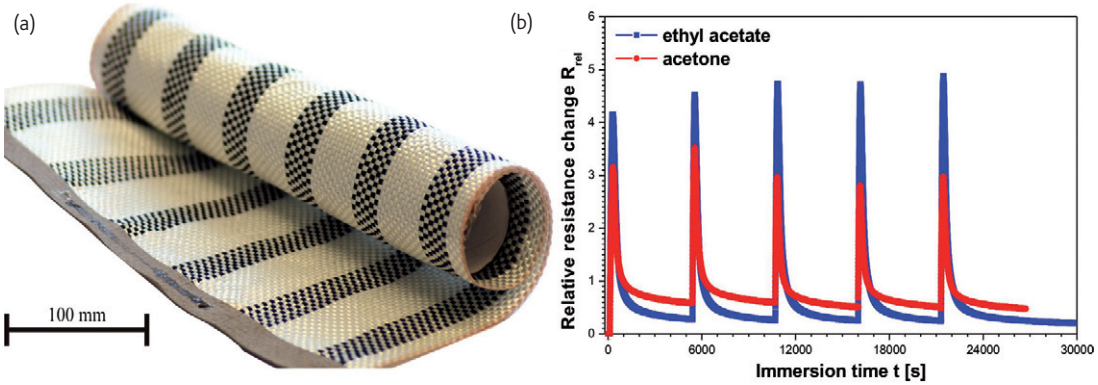

Fig. 4 Cyclic sensing experiments with sensory CPC textiles. (a) Prototype of a sensory CPC textile based on a PLA composite containing 3 wt.% MCWNT [PLA/MWCNT multifilament fibers produced by ENSAIT, France and textile weaving at TISSA Glasweberei AG, Switzerland]. (b) Electrical resistance change of a sensory CPC textile based on blend multifilament fibers of PLA/polycaprolactone blends with 3 wt.% MWCNT at cyclic contact with ethyl acetate and acetone, adapted from[27] with permission from Elsevier.

application, as polymers become stiffer with decreasing temperature. As the environmental temperature of industrial applications varies, the changing CPC response characteristic upon temperature changes has to be taken into account. Fig. 3b-III shows the temperature dependence of the diffusion coefficient *k*, which increases linearly with temperature. The data were again determined for a CPC/ethyl acetate system. The last aspect concerns the dependence of the diffusion coefficient *k* on the solvent concentration (Fig. 3b-IV). A linear decrease of the *k* value was found for decreasing solvent concentration, where a good solvent (chloroform) for PC was diluted with the bad solvents methanol or diethyl ether. This result indicates that the detection of partially polluted liquids like, e.g., water with organic solvents is possible.

All of the results presented on the electrical response characteristics of CPC immersed in organic solvents and the corresponding range of influencing factors underline the complexity of the material behavior. However, this complexity enables the design of highly precise CPC based sensors for the detection of numerous organic solvents within a very broad range of temperatures, with the capability to distinguish between different solvents.

Evaluation of a prototype CPC textile

Prototype CPC textiles containing multifilament fibers were used for experiments simulating real application conditions. For this purpose, polylactic acid (PLA)/MWCNT fibers were woven together with glass fiber textiles as shown in Fig. 4a. Although fiber spinning CPC still harbors technological challenges[31,32,35], sensory CPC fibers are very promising candidates for large-area sensor applications. Using the proposed CPC textile style also means that the cost-efficient

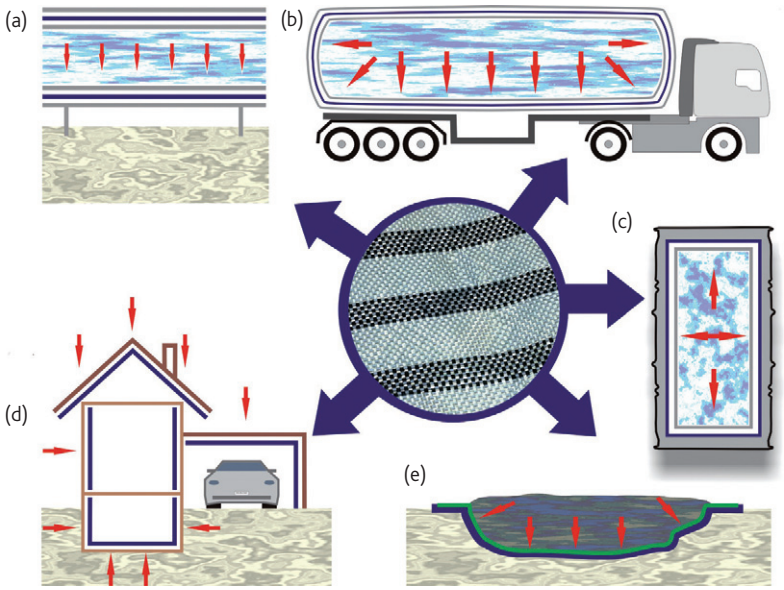

Fig. 5 Possible applications of sensory CPC textiles in building construction and industrial plants. (a) A piping system, (b) a tank on a truck, (a) a barrel, (d) buildings with flat and slanted roofs, and (e) a waste disposal site.

production of such sensors is possible. Due to the high surface to volume ratio of fibers, such textiles are characterized by fast response times and the ability to act as cyclic sensors. Fig. 4b shows cyclic sensing tests of a textile based on CPC multifilaments obtained from a blend system[27] in contact with different solvents. Thereby the textile was not fully immersed, but partially wetted with solvent drops. These results indicate that such textiles are very promising candidates for leakage detection.

Potential application fields

Fig. 5 shows some of the possible applications of sensory CPC textiles (dark blue lines) for building construction and industrial plants, where piping systems (Fig. 5a) and tanks have to be monitored. Mobile tanks in ships and trucks (Fig. 5b) as well as barrels (Fig. 5c), also located underground, can be surveyed. For building construction, sensory CPCs can be used for the detection of leakages in roofs and basement walls (Fig. 5d), where rain and groundwater can lead to serious damage. Another interesting application could be the monitoring of waste disposal sites (Fig. 5e), where the contamination of the ground water has to be avoided. Sensory CPC textiles can provide reliable and locally resolved analysis of leakages in barrier sheets. The detection of organic solvent leakages of tanks and piping systems, may use sensory textiles as cladding.

Outlook

The use of smart polymer/CNT composites in leakage detection is very promising, due to the combined technological and economical benefits. Such sensory CPCs containing CNTs can be realized using tailored, cost-efficient melt processing techniques that are already used in industry, such as injection or blow molding, and fiber spinning. Due to this variety of molding techniques they can made into nearly every imaginable shape, meaning they can be incorporated into the existing structural components of buildings or industrial plants. As we develop a more comprehensive understanding of the fundamental issues regarding the sensing mechanism and composite processing, the transfer of laboratory scale sensors to real industrial applications becomes possible. mt

Instrument citation

DMM2000 multimeter, Keithley

Acknowledgement

The development of conductive composites and textiles containing CNTs for different sensing applications, like strain, temperature, vapor and solvent sensing, was the main topic of the a European Integrated Project supported through the Sixth Framework Programme for Research and Technological development named INTELTEX (Intelligent multi-reactive textiles integrating nanofiller based CPC-fibres). The authors are grateful for financial support within that project. In addition, thanks is given to Nanocyl S.A. for leading the project and providing the nanotubes and the project partners Université de Bretagne-Sud (UBS), Queen Mary University of London (QMUL), Ecole Nationale Supérieure des Arts et Industries Textiles (ENSAIT), and Universidade do Minho (UMINHO) for the scientific exchange. TISSA Glasweberei AG, Switzerland is gratefully thanked for the weaving of CPC textiles.

REFERENCES

1. Narkis, M., *et al.*, *Synth Met* (2000) **113**(1-2), 29.
2. Segal, E., *et al.*, *Polym Eng Sci* (2002) **42**(12), 2430.
3. Segal, E., *et al.*, *J Polym Sci Pt B-Polym Phys* (2003) **41**(12), 1428.
4. Srivastava, S., *et al.*, *Polym Eng Sci* (2000) **40**(7), 1522.
5. Tsubokawa, N., *et al.*, *Sensor Actuat B-Chem* (2001) **79**(2-3), 92.
6. S.G. Chen, S. G., *et al.*, *Sensor Actuat B-Chem* (2005) **105**(2), 187.
7. Feller, J. F., and Grohens, Y., *Synth Met* (2005) **154**(1-3), 193.
8. Li, J. R., *et al.*, *Compos Sci Technol* (2006) **66**(16), 3126.
9. Quercia, L., *et al.*, *Sensor Actuat B-Chem* (2004) **100**(1-2), 22.
10. Quercia, L., *et al.*, *Sensor Actuat B-Chem* (2005) **109**(1), 153.
11. Xie, H. F., *et al.*, *Sensor Actuat B-Chem* (2006) **113**(2), 887.
12. Iijima, S., *Nature* (1991) **354**(6348), 56.
13. Jin, Z., *et al.*, *Chem Phys Lett* (2001) **337**(1-3), 43.
14. Qian, D., *et al.*, *Appl Phys Lett* (2000) **76**(20), 2868.
15. Li, C., *et al.*, *Compos Sci Technol* (2008) **68**(6), 1227.
16. Wei, C., *et al.*, *J Am Chem Soc* (2006) **128**(5), 1412.
17. Fan, Q., *et al.*, *Sensor Actuat B-Chem*, (2011) **156**(1), 63.
18. Castro, M., *et al.*, *Carbon* (2009) **47**(8), 1930.
19. Philip, B., *et al.*, *Smart Mater Struct* (2003) **12**(6), 935.
20. Yoon, H., *et al.*, *Smart Mater Struct* (2006) **15**(1), S14.
21. Luo, Y. L., *et al.*, *Synth Met* (2007) **157**(8-9), 390.
22. Zhang, B., *et al.*, *Sensor Actuat B-Chem* (2005) **109**(2), 323.
23. Kobashi, K., *et al.*, *Smart Mater Struct* (2009) **18**(3), 035008.1.
24. Kobashi, K., *et al.*, *Sensor Actuat B-Chem* (2008) **134**(2), 787.
25. Pötschke, P., *et al.*, *Compos Sci Technol* (2010) **70**(2), 343.
26. Pötschke, P., *et al.*, *Compos Sci Technol, submitted* (2010).
27. Rentenberger, R., *et al.*, *Sensor Actuat B-Chem*, doi: 10.1016/j.compscitech.2011.05.019.
28. Villmow, T., *et al.*, *Polymer* (2011) **52**(10), 2276.
29. Du, F. M., *et al.*, *Phys Rev B* (2005) **72**(12), 121404(R).
30. Haggenmueller, R., *et al.*, *Chem Phys Lett* (2000) **330**(3-4), 219.
31. Pötschke, P., *et al.*, *Polymer* (2005) **46**(23), 10355.
32. Fornes, T. D., *et al.*, *Polymer* (2006) **47**(5), 1704.
33. Li, *et al.*, Q., *Compos Part B Eng* (2009) **40**(3), 218.
34. He, *et al.*, X. J., *Appl Phys Lett* (2005) **86**(6), 062112.
35. Badaire, S., *et al.*, *J Appl Phys* (2004) **96**(12), 7509.
36. Kymakis, E., and Amaratunga, G. A. J., *J Appl Phys* (2006) **99**(8), 084302-1.
37. Miaudet, P., *et al.*, *Polymer* (2007) **48**(14), 4068.
38. Bilotti, E., *et al.*, *J Mater Chem* (2010) **20**(42), 9449.
39. Li, C. Y., *et al.*, *Appl Phys Lett* (2007) **91**(22), 218.
40. Hildebrand, J. H., and Scott, R. L., *The solubility of nonelectrolytes*, Reinhold Pub. Corp., 1950.
41. Hildebrand, J. H., and Scott, R. L., *Regular solutions*, Prentice-Hall, 1962.
42. Hansen, C. M., *Hansen solubility parameters: a user's handbook*, CRC Press, 2007.
43. Brandrup, J., *et al.*, *Polymer handbook*, Wiley, 1999.